

## Residual stresses in a finite cylinder. Direct and inverse problems and their solving using the variational method of homogeneous solutions

Chekurin V., Postolaki L.

*Pidstryhach Institute for Applied Problems of Mechanics and Mathematics  
National Academy of Sciences of Ukraine,  
3-b Naukova Str., Lviv, 79060, Ukraine*

(Received 20 September 2018)

Mathematical models and methods for determination of axisymmetric residual stresses in a finite cylinder are considered. The model of residual stresses is built using the conception of incompatible eigenstrain tensor. Within the frame of this model, a direct problem for residual stresses determination is formulated. A method based on the variational method of homogeneous solutions is developed for solving the direct problem. Using the obtained solution, features of residual stresses, caused by continuous and piece-wise homogeneous distributions of eigenstrain components are studied. A variational formulation of the inverse problem for residual stresses determination on the base of empirical data obtained by a photoelasticity method is suggested. The inverse problem is solved numerically with the use of iterative calculations of values of the criterion functional. The results presented in the paper can be used for the development of methods and means for nondestructive testing and engineering characterization of materials and structural elements.

**Keywords:** *residual stresses, finite cylinder, photoelasticity, direct and inverse problems, variational method of homogeneous solutions.*

**2000 MSC:** 35J30

**UDC:** 539.3

**DOI:** 10.23939/mmc2018.02.119

### 1. Introduction

Residual stresses exist in solid bodies, regardless of the presence of external force or thermal loadings [1]. These stresses arise in various solid materials, such as metals, glasses, ceramics, semiconductors, some plastics, fabricated upon high-temperature heating and quick cooling down. Residual stresses aroused in structure elements, being superimposed on external stresses, can influence the properties of these elements, such as strength, thermal-shock resistance, durability etc. Hence, development of effective methods for residual stresses determination in solids is a problem of great scientific and applied importance.

There are various methods for determination of residual stresses in solids. Depending on their impact on the object, one can consider destructive (for example, block removal, splitting and layering, the contour method), semi-destructive (centre-hole and deep-hole drilling, and the ring core method etc.) techniques, as well nondestructive ones. The last group of techniques includes those based on empirical information obtaining upon probing the object by external fields. These are X-ray and neutron diffraction, magnetic, optical and ultrasonic methods etc. [1, 2].

The nondestructive theoretical-experimental methods, based on models of interaction of external physical fields with stress fields in strained solids, often can be brought to inverse problems, the input data for which can be obtained from physical measuring [3, 4]. In photoelasticity methods, for instance, polarized light is used as external probing field. Models of integrated photoelasticity [5, 6] establish relationships between polarization parameters of probing light ray and distributions of strain or/and stress tensor components along the path of its propagation within the object. Measuring the states of light polarization at the input and output of the object and applying corresponding photoelasticity

mathematical model, one can obtain some integral a posteriori information about the strain-stressed state along the probing ray. Scanning the object by the ray in different directions, one can obtain the data, amount of which is sufficient for complete restoration of objective strain-stressed state, and formulate on this basis a corresponding inverse problem. Implementation of such approach can vary, depending on applied mathematical models for residual stresses and interaction of probing rays with stress field, as well as on the empirical data, used as input ones.

A mathematical models and methods for axisymmetric residual stresses determination in a finite cylinder are considered in the paper. The residual stresses are modeled with the use of known eigenstrain conception [7]. A direct problem for residual stresses determination is formulated in the frame of this model. The components of eigenstrain tensor are considered as given functions in this problem. It is solved with the use of the variational method of homogeneous solutions [8,9]. On this basis features of residual stresses are studied for some distributions of eigenstrain tensor components prescribed in the body volume.

An inverse problem is formulated in the frames of the model of residual stresses and the model of integrated photoelasticity. The components of both residual stress tensor and eigenstrain tensor are considered here as unknown functions. To make the problem closed, it is supplemented with empirical data, which can be obtained with the use of probing the cylinder by polarized light. Three constituents — a mathematical model for residual stresses, a mathematical model for polarized light interaction with stress field, and empirical data are united through variational formulation of the inverse problem. For that a functional, which determines the mean square deviation of an arbitrary solution of the direct problem from the given empirical data, was constructed. A method for inverse problem solving was developed with the use of the variational method of homogeneous solutions. The convergence of the method and precision of the obtained solutions were studied with the use of numerical experiments.

## 2. A mathematical model for axisymmetric residual stresses in the cylinder

Consider the elastic body  $\mathbf{B}$  in the form of the finite cylinder  $V = (0 \leq \rho \leq 1, 0 \leq \varphi \leq 2\pi, -b \leq z \leq b)$ , which rests in axisymmetric stressed state. Here  $\rho, \varphi, z$  stand for cylindrical coordinates ( $\rho$  and  $z$  are correspondingly the dimensionless radial and axial coordinates normalized to radius  $R$  of the cylinder). The surface  $\partial V = S_1 \cup S \cup S_2$  of the cylinder, where  $S = (\rho = 1, 0 \leq \varphi \leq 2\pi, -b \leq z \leq b)$ ,  $S_1 = (0 \leq \rho \leq 1, 0 \leq \varphi \leq 2\pi, z = -b)$ ,  $S_2 = (0 \leq \rho \leq 1, 0 \leq \varphi \leq 2\pi, z = b)$ , is traction-free:

$$\sigma_{\rho\rho}|_{\rho=1} = 0, \quad \sigma_{\rho z}|_{\rho=1} = 0, \quad \sigma_{zz}|_{z=\pm b} = 0, \quad \sigma_{\rho z}|_{z=\pm b} = 0, \quad (1)$$

where  $\sigma_{\rho\rho}, \sigma_{zz}, \sigma_{\varphi\varphi}, \sigma_{\rho z}$  stand for the components of the axisymmetric stress tensor in cylindrical coordinates.

The axisymmetric stressed state of the body is caused by structural inhomogeneity of the material. One can take it into account through representation of the total strain tensor  $e_{ij}$  as the sum of elastic strain  $e_{ij}^e$  and eigenstrain  $\hat{e}_{ij}$  [9]:

$$e_{ij} = e_{ij}^e + \hat{e}_{ij}, \quad ij \in \{\rho\rho, zz, \varphi\varphi, \rho z\}. \quad (2)$$

The components  $e_{ij}$  of the total strain tensor  $\mathbf{e}$  are compatible. They can be determined in the terms of the radial  $u_\rho$  and axial  $u_z$  components of dimensionless displacement vector<sup>1</sup>  $\mathbf{u} \leftarrow \mathbf{u}/R$  by Cauchy's relations [10]:

$$e_{\rho\rho} = \frac{\partial u_\rho}{\partial \rho}, \quad e_{zz} = \frac{\partial u_z}{\partial z}, \quad e_{\varphi\varphi} = \frac{u_\rho}{\rho}, \quad e_{\rho z} = \frac{1}{2} \left( \frac{\partial u_\rho}{\partial z} + \frac{\partial u_z}{\partial \rho} \right). \quad (3)$$

<sup>1</sup>Here and further for simplicity of notation, we use the same letter for normalized quantity as for the initial one.

The components  $e_{ij}^e$  of elastic strain and eigenstrain  $\hat{e}_{ij}$  tensors are incompatible. Hence, we cannot associate them with some displacements. But we can link the elastic strain components  $e_{ij}^e$  to stress tensor components  $\sigma_{ij}$ . Corresponding elasticity relations for the case of axisymmetry have the form

$$\begin{aligned}\sigma_{\rho\rho} &= \frac{E}{(1+\nu)(1-2\nu)} \left( (1-\nu)e_{\rho\rho}^e + \nu(e_{zz}^e + e_{\varphi\varphi}^e) \right), \\ \sigma_{zz} &= \frac{E}{(1+\nu)(1-2\nu)} \left( (1-\nu)e_{zz}^e + \nu(e_{\rho\rho}^e + e_{\varphi\varphi}^e) \right), \\ \sigma_{\varphi\varphi} &= \frac{E}{(1+\nu)(1-2\nu)} \left( (1-\nu)e_{\varphi\varphi}^e + \nu(e_{zz}^e + e_{\rho\rho}^e) \right), \\ \sigma_{\rho z} &= \frac{E}{1+\nu} e_{\rho z}^e.\end{aligned}\quad (4)$$

Here  $\nu$  and  $E$  stand for the Poisson ratio and Young's module of the material.

The components  $\sigma_{\rho\rho}$ ,  $\sigma_{zz}$ ,  $\sigma_{\varphi\varphi}$ ,  $\sigma_{\rho z}$  of the stress tensor satisfy the equilibrium equation [10]:

$$\begin{aligned}\frac{1}{\rho} \frac{\partial}{\partial \rho} (\rho \sigma_{\rho\rho}) + \frac{\partial}{\partial z} \sigma_{\rho z} - \frac{1}{\rho} \sigma_{\varphi\varphi} &= 0, \\ \frac{1}{\rho} \frac{\partial}{\partial \rho} (\rho \sigma_{\rho z}) + \frac{\partial}{\partial z} \sigma_{zz} &= 0.\end{aligned}\quad (5)$$

Further we restrict our consideration by the case, when all three non-zero eigenstrain components  $\hat{e}_{\rho\rho}$ ,  $\hat{e}_{\varphi\varphi} = \hat{e}_{\rho\rho}$  and  $\hat{e}_{zz}$  depend only on the radial coordinate  $\rho$  and present them in the form:

$$\hat{e}_{\rho\rho}(\rho) = \hat{e}_1^0 \hat{e}_1(\rho), \quad \hat{e}_{\varphi\varphi}(\rho) = \hat{e}_1^0 \hat{e}_1(\rho), \quad \hat{e}_{zz}(\rho) = \hat{e}_2^0 \hat{e}_2(\rho), \quad (6)$$

where  $\hat{e}_1^0$ ,  $\hat{e}_2^0$  are some real constants,  $\hat{e}_1(\rho)$  and  $\hat{e}_2(\rho)$  are differentiable functions ranged in segment  $[0, 1]$ :  $\hat{e}_1(\rho), \hat{e}_2(\rho) \in [0, 1] \forall \rho \in [0, 1]$ .

With the use of relationship (2), one can express stress components  $\sigma_{ij}$  in term of total strain  $e_{ij}$  and eigenstrain components:

$$\begin{aligned}\sigma_{\rho\rho} &= \frac{1}{(1+\nu)(1-2\nu)} \left( (1-\nu)e_{\rho\rho} + \nu(e_{zz} + e_{\varphi\varphi}) \right) - \frac{1}{1-2\nu} \hat{e}_0 \hat{e}_1(\rho), \\ \sigma_{zz} &= \frac{1}{(1+\nu)(1-2\nu)} \left( (1-\nu)e_{zz} + \nu(e_{\rho\rho} + e_{\varphi\varphi}) \right) - \frac{1}{1-2\nu} \hat{e}_2(\rho), \\ \sigma_{\varphi\varphi} &= \frac{1}{(1+\nu)(1-2\nu)} \left( (1-\nu)e_{\varphi\varphi} + \nu(e_{zz} + e_{\rho\rho}) \right) - \frac{1}{1-2\nu} \hat{e}_0 \hat{e}_1(\rho), \\ \sigma_{\rho z} &= \frac{1}{1+\nu} e_{\rho z}.\end{aligned}\quad (7)$$

Here  $\sigma_{ij}$  and  $e_{ij}$  are already normalized components:  $\sigma_{ij} \leftarrow \sigma_{ij}/E\hat{e}_2^0$  and  $e_{ij} \leftarrow e_{ij}/\hat{e}_2^0$ ;  $\hat{e}_0 = \hat{e}_1^0/\hat{e}_2^0$ .

Expressing  $e_{ij}$  in (7) via  $u_\rho$  and  $u_z$  in correspondence with (3), and substituting the obtained relations into the equilibrium equations (5), we come to the equations in term of displacements:

$$\begin{aligned}\nabla^2 u_\rho + \frac{1}{1-2\nu} \frac{\partial e}{\partial \rho} - \frac{u_\rho}{\rho^2} &= \hat{e}_0 \frac{2(1+\nu)}{1-2\nu} \frac{d\hat{e}_1(\rho)}{d\rho}, \\ \nabla^2 u_z + \frac{1}{1-2\nu} \frac{\partial e}{\partial z} &= 0,\end{aligned}\quad (8)$$

where  $e = e_{\rho\rho} + e_{zz} + e_{\varphi\varphi}$ ,  $\nabla^2 = \partial^2/\partial\rho^2 + \rho^{-1}\partial/\partial\rho + \partial^2/\partial z^2$  is axisymmetric Laplace operator.

Expressing the boundary conditions (1) in term of displacement components with the use of relationships (7), we obtain

$$\begin{aligned} \frac{\partial u_\rho}{\partial \rho} \Big|_{\rho=1} + \frac{\nu}{1-\nu} \left( \frac{\partial u_z}{\partial z} \Big|_{\rho=1} + u_\rho \Big|_{\rho=1} \right) &= \frac{1+\nu}{1-\nu} \hat{e}_0 \hat{e}_1 \Big|_{\rho=1}, & \frac{\partial u_\rho}{\partial z} \Big|_{\rho=1} + \frac{\partial u_z}{\partial \rho} \Big|_{\rho=1} &= 0, \\ \frac{\partial u_z}{\partial z} \Big|_{z=\pm b} + \frac{\nu}{1-\nu} \left( \frac{\partial u_\rho}{\partial \rho} \Big|_{z=\pm b} + \frac{u_\rho}{\rho} \Big|_{z=\pm b} \right) &= \frac{1+\nu}{1-\nu} \hat{e}_0 \hat{e}_1(\rho), & \frac{\partial u_\rho}{\partial z} \Big|_{z=\pm b} + \frac{\partial u_z}{\partial \rho} \Big|_{z=\pm b} &= 0. \end{aligned} \quad (9)$$

The equations (8) and the boundary conditions (9) form a mathematical model for axisymmetric residual stresses in the cylinder in the case, when eigenstrain components are depending only on a radial coordinate.

### 3. The direct problem for residual stresses determination and a method for its solving

#### 3.1. A solution presentation

In the direct problem, we assume the eigenstrain components  $\hat{e}_{\rho\rho}(\rho) = \hat{e}_{\varphi\varphi}(\rho)$ ,  $\hat{e}_{zz}(\rho)$  to be known functions. Solving the boundary value problem (8), (9), one can determine the components  $u_\rho$  and  $u_z$  of the displacement vector, and then, using the relations (3) and (7), calculate the stress components  $\sigma_{\rho\rho}$ ,  $\sigma_{zz}$ ,  $\sigma_{\varphi\varphi}$ ,  $\sigma_{\rho z}$ .

We present the solution of the inhomogeneous problem (8), (9) as the sum [9]:

$$u_\rho(\rho, z) = u_\rho^0(\rho) + \tilde{u}_\rho(\rho, z), \quad u_z(\rho, z) = u_z^0(\rho) + \tilde{u}_z(\rho, z). \quad (10)$$

Here  $\{u_\rho^0(\rho), u_z^0(\rho)\}$  is the solution of the inhomogeneous system (8) for an infinite unloaded cylinder resting in the state of plane strain. We call it the solution of the initial state. In this case, the second equation (5) is satisfied identically and the first one brings to an ordinary differential equation:

$$\frac{d}{d\rho} \left[ \frac{1}{\rho} \frac{d(\rho u_\rho^0(\rho))}{d\rho} \right] + \frac{\nu}{1-\nu} \frac{de_{zz}^0(\rho)}{d\rho} = \hat{e}_0 \frac{1+\nu}{1-\nu} \frac{d\hat{e}_1(\rho)}{d\rho}. \quad (11)$$

It should be subordinated to the conditions of external loading lack:

$$\sigma_{\rho\rho}^0 \Big|_{\rho=1} = 0, \quad \int_0^1 \rho \sigma_{zz}^0 d\rho = 0. \quad (12)$$

The pair  $\{\tilde{u}_r(\rho, z), \tilde{u}_z(\rho, z)\}$  represents the solution of the boundary-value problem for homogeneous system corresponding to the system (8):

$$\begin{aligned} \nabla^2 \tilde{u}_\rho + \frac{1}{1-2\nu} \frac{\partial \tilde{e}}{\partial \rho} - \frac{\tilde{u}_\rho}{\rho^2} &= 0, \\ \nabla^2 \tilde{u}_z + \frac{1}{1-2\nu} \frac{\partial \tilde{e}}{\partial z} &= 0, \end{aligned} \quad (13)$$

where  $\tilde{e} = \tilde{e}_{\rho\rho} + \tilde{e}_{zz} + \tilde{e}_{\varphi\varphi}$ , with the boundary conditions

$$\tilde{\sigma}_{\rho\rho} \Big|_{\rho=1} = 0, \quad \tilde{\sigma}_{\rho z} \Big|_{\rho=1} = 0, \quad \tilde{\sigma}_{zz} \Big|_{z=\pm b} = -\sigma_{zz}^0, \quad \tilde{\sigma}_{\rho z} \Big|_{z=\pm b} = 0, \quad (14)$$

where  $\sigma_{zz}^0$  is the axial stress component, which corresponds to the solution  $\{u_\rho^0(\rho), u_z^0(\rho)\}$ .

We call  $\{\tilde{u}_r(\rho, z), \tilde{u}_z(\rho, z)\}$  the solution for the disturbed state.

### 3.2. Solving the initial problem

Integrating the equation (11) and taking into account the condition of stress finiteness, we obtain

$$u_\rho^0 = \hat{e}_0 \frac{1+\nu}{1-\nu} \frac{1}{\rho} \int_0^\rho \rho \hat{e}_1(\rho) d\rho - \frac{\nu}{1-\nu} \frac{1}{\rho} \int_0^\rho \rho e_{zz}^0(\rho) d\rho + \frac{\rho}{2} C_1, \quad (15)$$

where  $C_1$  is an integration constant.

Then, using the relations (3)<sub>1...3</sub> and (7)<sub>2</sub>, one can calculate the stress component  $\sigma_{zz}^0$ . Subordinating it to the conditions (12), we obtain

$$C_1 = \frac{2}{(\nu-1)} \int_0^1 (\hat{e}_0(\nu-1)\hat{e}_1(\rho) + \nu \hat{e}_2(\rho)) \rho d\rho, \quad (16)$$

$$e_{zz}^0(\rho) = \frac{2\hat{e}_0 \nu \hat{e}_1(\rho) - \hat{e}_2(\rho)}{2\nu-1}. \quad (17)$$

Finally, we come to the next formulas for the components  $\sigma_{\rho\rho}^0$ ,  $\sigma_{zz}^0$ ,  $\sigma_{\varphi\varphi}^0$  of residual stresses in the initial state:

$$\begin{aligned} \sigma_{\rho\rho}^0 &= \frac{1}{(1-\nu^2)(2\nu-1)} \left( \int_0^1 F(\rho) \rho d\rho - \frac{1}{\rho^2} \int_0^\rho F(\rho) \rho d\rho \right), \\ \sigma_{zz}^0 &= \frac{\nu}{(1-\nu^2)(2\nu-1)} \left( 2 \int_0^1 F(\rho) \rho d\rho - F(\rho) \right), \\ \sigma_{\varphi\varphi}^0 &= \frac{1}{(1-\nu^2)(2\nu-1)} \left( \int_0^1 F(\rho) \rho d\rho + \frac{1}{\rho^2} \int_0^\rho F(\rho) \rho d\rho - F(\rho) \right). \end{aligned} \quad (18)$$

Here  $F(\rho) = \hat{e}_0(\nu-1)\hat{e}_1(\rho) + \nu \hat{e}_2(\rho)$ .

### 3.3. Solving the disturbed problem by variational method of homogeneous solutions

With the use of the Love function [10], the system (13) is reduced to the biharmonic equation:

$$\nabla^2 \nabla^2 \chi = 0. \quad (19)$$

Components of the displacement vector  $\tilde{u}_\rho$ ,  $\tilde{u}_z$  and the stress tensor  $\tilde{\sigma}_{ij}$ ,  $ij \in (\rho\rho, zz, \varphi\varphi, \rho z)$  can be expressed in term of the Love function  $\chi$  as follows [10]:

$$\tilde{u}_\rho = -\frac{\partial^2 \chi}{\partial \rho \partial z}, \quad \tilde{u}_z = \frac{\partial^2 \chi}{\partial z^2} + 2(1-\nu) \nabla^2 \chi, \quad (20)$$

$$\begin{aligned} \frac{1}{2\mu} \tilde{\sigma}_{\rho\rho} &= \frac{\partial}{\partial z} \left( \nu \nabla^2 \chi - \frac{\partial^2 \chi}{\partial \rho^2} \right), & \frac{1}{2\mu} \tilde{\sigma}_{zz} &= \frac{\partial}{\partial z} \left( (2-\nu) \nabla^2 \chi - \frac{\partial^2 \chi}{\partial z^2} \right), \\ \frac{1}{2\mu} \tilde{\sigma}_{\varphi\varphi} &= \frac{\partial}{\partial z} \left[ \nu \nabla^2 \chi - \frac{1}{\rho} \frac{\partial \chi}{\partial \rho} \right], & \frac{1}{2\mu} \tilde{\sigma}_{\rho z} &= \frac{\partial}{\partial \rho} \left( (1-\nu) \nabla^2 \chi - \frac{\partial^2 \chi}{\partial z^2} \right). \end{aligned} \quad (21)$$

Here  $\mu = E/2(1+\nu)$  is the shear modulus.

The solution of the problem (19), (14), obtained with the use of variational method of homogeneous solutions, is presented in the paper [8]. For the considered here case of symmetry, with respect to the plan  $z=0$ , strain-stressed state, the solution of equation (19) can be presented in the form:

$$\chi = \frac{1}{2} \sum_{k=1}^{\infty} (B_k \sinh(-\gamma_k z) f_k(\rho) + \bar{B}_k \sinh(-\bar{\gamma}_k z) \bar{f}_k(\rho)), \quad (22)$$

where  $B_k, \bar{B}_k, k = 1, 2, \dots$  are undetermined complex constants (the overlined symbols denote here and further the corresponding complex conjugate parameters),  $f_k(\rho)$  are the radial functions, expressed through Bessel functions  $J_0$  and  $J_1$  as:

$$f_k(\rho) = \left( \rho J_1(\gamma_k \rho) \kappa_k - \frac{2}{\pi \gamma_k} J_0(\gamma_k \rho) \right),$$

$\gamma_k$  are complex roots of the transcendental equation

$$\gamma_k^2 (J_0^2(\gamma_k) + J_1^2(\gamma_k)) + 2(\nu - 1) J_1^2(\gamma_k) = 0,$$

$\varkappa_k$  are complex constants

$$\varkappa_k = \frac{2J_1(\gamma_k)}{\pi((2\nu - 2)J_1(\gamma_k) - \gamma_k J_0(\gamma_k))}.$$

Substituting the Love function (22) into the relationships (21), one can obtain the presentation for the stress components of the disturbed state:

$$\begin{aligned} \tilde{\sigma}_{\rho\rho}(\rho, z) &= \frac{1}{2} \sum_{k=1}^{\infty} (B_k \cosh(\gamma_k z) \sigma_{k\rho\rho}(\rho) + \bar{B}_k \cosh(\bar{\gamma}_k z) \bar{\sigma}_{k\rho\rho}(\rho)), \\ \tilde{\sigma}_{\varphi\varphi}(\rho, z) &= \frac{1}{2} \sum_{k=1}^{\infty} (B_k \cosh(\gamma_k z) \sigma_{k\varphi\varphi}(\rho) + \bar{B}_k \cosh(\bar{\gamma}_k z) \bar{\sigma}_{k\varphi\varphi}(\rho)), \\ \tilde{\sigma}_{zz}(\rho, z) &= \frac{1}{2} \sum_{k=1}^{\infty} (B_k \cosh(\gamma_k z) \sigma_{kzz}(\rho) + \bar{B}_k \cosh(\bar{\gamma}_k z) \bar{\sigma}_{kzz}(\rho)), \\ \tilde{\sigma}_{\rho z}(\rho, z) &= \frac{1}{2} \sum_{k=1}^{\infty} (B_k \sinh(\gamma_k z) \sigma_{k\rho z}(\rho) + \bar{B}_k \sinh(\bar{\gamma}_k z) \bar{\sigma}_{k\rho z}(\rho)). \end{aligned} \quad (23)$$

Here  $\sigma_{k\rho\rho}, \sigma_{k\varphi\varphi}, \sigma_{kzz}$  and  $\sigma_{k\rho z}, k = 1, 2, \dots$  are systems of homogeneous solutions:

$$\begin{aligned} \sigma_{k\rho\rho}(\rho) &= 2\mu\gamma_k \left( (\nu - 1)f_k''(\rho) + \frac{\nu}{\rho}f_k'(\rho) + \nu\gamma_k^2 f_k(\rho) \right), \\ \sigma_{k\varphi\varphi}(\rho) &= 2\mu\gamma_k \left( \nu f_k''(\rho) + \frac{\nu - 1}{\rho}f_k'(\rho) + \nu\gamma_k^2 f_k(\rho) \right), \\ \sigma_{kzz}(\rho) &= 2\mu\gamma_k \left( (2 - \nu) \left( f_k''(\rho) + \frac{1}{\rho}f_k'(\rho) \right) + (1 - \nu)\gamma_k^2 f_k(\rho) \right), \\ \sigma_{k\rho z}(\rho) &= 2\mu \left( (1 - \nu) \left( f_k'''(\rho) + \frac{1}{\rho}f_k''(\rho) \right) + \left( (1 - \nu) \left( \gamma_k^2 - \frac{1}{\rho} \right) - \gamma_k^2 \right) f_k'(\rho) \right), \end{aligned} \quad (24)$$

which satisfy the homogeneous conditions on the cylindrical surface of the body:

$$\sigma_{k\rho\rho}|_{\rho=1} = 0, \quad \sigma_{k\rho z}|_{\rho=1} = 0, \quad \forall k = 1, 2, \dots \quad (25)$$

Therefore the solution in the form (23) satisfies the first two boundary conditions (14), imposed on the lateral surface of the cylinder, automatically for any values of the coefficients  $B_k$ .

To subordinate the solution to another two boundary conditions, one can choose appropriately the infinite sequence of the constants  $B_k$ . As  $B_k$  are complex constants, it makes possible to satisfy both conditions (14), prescribed on the bases of the cylinder. We use for that the variational approach [8, 11].

Let us consider the functional:

$$F = \int_0^1 \left[ (\bar{\sigma}_{zz}|_{z=b} + \sigma_{zz}^0(\rho))^2 + (\bar{\sigma}_{\rho z}|_{z=b})^2 \right] \rho d\rho. \quad (26)$$

It determines in  $L_2$  norm the deviation of the solution (23) from boundary data, prescribed on the bases of the cylinder by conditions (14)<sub>3</sub> and (14)<sub>4</sub>. The necessary conditions of minimum of the functional:

$$\frac{\partial F}{\partial B_m} = 0, \quad \frac{\partial F}{\partial \bar{B}_m} = 0, \quad m = 1, 2, \dots$$

brings the infinite system of linear algebraic equations:

$$\sum_{k=1}^{\infty} \sum_{p=1}^2 M_{mk}^{lp} B_k^p = K_m^l, \quad m = 1, 2, \dots \quad (27)$$

where  $B_k^1 \equiv B_k$ ,  $B_k^2 \equiv \bar{B}_k$  and the coefficients  $M_{mk}^{lp}$ ,  $K_m^l$ , ( $l = 1, 2$ ;  $m = 1, 2, \dots$ ) of the system (27) are defined by the formulas:

$$M_{mk}^{lp} = \frac{1}{2} \int_0^1 \left( \sigma_{kzz}^p(\rho) \sigma_{mzz}^l(\rho) + \sigma_{k\rho z}^p(\rho) \sigma_{m\rho z}^l(\rho) \right) \rho d\rho, \quad (28)$$

$$K_m^l = - \int_0^1 \left( \sigma_{zz}^0(\rho) \sigma_{mzz}^l(\rho) \right) \rho d\rho. \quad (29)$$

We used the notations in the formulas (28), (29):

$$\sigma_{kzz}^1(\rho) \equiv \cosh(\gamma_k b) \sigma_{kzz}(\rho), \quad \sigma_{kzz}^2(\rho) \equiv \cosh(\bar{\gamma}_k b) \bar{\sigma}_{kzz}(\rho),$$

$$\sigma_{k\rho z}^1(\rho) \equiv \sinh(\gamma_k b) \sigma_{k\rho z}(\rho), \quad \sigma_{k\rho z}^2(\rho) \equiv \sinh(\bar{\gamma}_k b) \bar{\sigma}_{k\rho z}(\rho).$$

Solving the linear system (27), one can find the coefficients  $B_k$ ,  $\bar{B}_k$  and calculate by the formulas (23) the components of the stress tensor in the disturbed state.

Finally, one can determine the residual stresses in the cylinder as

$$\sigma_{ij}(\rho, z) = \sigma_{ij}^0(\rho) + \bar{\sigma}_{ij}(\rho, z), \quad ij \in \{\rho\rho, zz, \varphi\varphi, \rho z\}. \quad (30)$$

#### 4. Numerical study of the direct problem

The obtained solution (30) has practical value, when functions of eigenstrain components are given. In this case, the problem is well defined. We can determine the stress components of the initial state, performing integration in the formulas (18), and stress components of the disturbed state by solving the infinite system, using one of the appropriate methods, for instance — the method of reduction [12].

If the reduction method is used, one should solve the finite system

$$\sum_{k=1}^N \sum_{p=1}^2 M_{mk}^{lp} B_k^p = K_m^l \quad (31)$$

instead of the system (27).

One can come to the system (31) by taking in the expansion (22) only the  $N$  first terms. Inaccuracy of the obtained solution can be evaluated numerically by the value of the functional (26) calculated for it. The convergence of the solution, obtaining with the use of reduction method, can be evaluated by

investigation of how the value of the functional is changing with increasing of the number  $N$ . Results of such studies, conducted earlier, are presented in the paper [8, 11].

The functions  $\hat{e}_1(\rho)$  and  $\hat{e}_2(\rho)$ , which define the eigenstrain components, can be chosen from the class of square-integrable functions. We have studied the solutions for two representatives of this class — a continuous function and a piece-wise continuous one. We restricted ourselves by the case of isotropic eigenstrain tensor, when

$$\hat{e}_2(\rho) = \hat{e}_1(\rho) \equiv \hat{e}(\rho) \quad (32)$$

and considered two types functions  $\hat{e}(\rho)$ :

$$\hat{e}(\rho) = \exp\left(\frac{\rho-1}{a}\right) \quad \text{and} \quad \hat{e}(\rho) = \begin{cases} \varepsilon, & \rho \leq \rho_1, \\ 1, & \rho > \rho_1. \end{cases} \quad (33)$$

The graphs of the dimensionless stress components  $\sigma_{\rho\rho}^0$ ,  $\sigma_{\varphi\varphi}^0$ ,  $\sigma_{zz}^0$  (curves 1 to 3 correspondingly) in the initial state as the functions of radial coordinate are shown in Fig. 1 for the cases of continuous (a) and piece-wise homogeneous (b) eigenstrain functions (33).

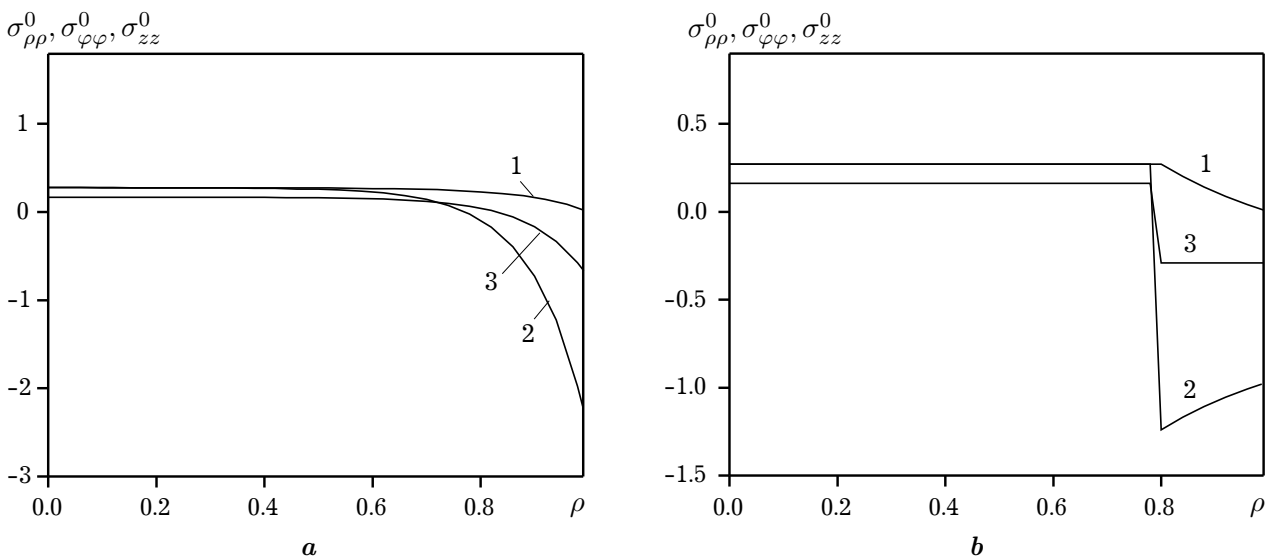


**Fig. 1.** Radial dependencies of stress component  $\sigma_{\rho\rho}^0$ ,  $\sigma_{\varphi\varphi}^0$ ,  $\sigma_{zz}^0$  (curves 1 to 3 correspondingly) for the cases of continuous (a) and piece-wise homogeneous (b) eigenstrain functions  $\hat{e}(\rho)$ .

The presented curves were calculated for  $\nu = 0.3$ ,  $a = 0.1$ ,  $\varepsilon = 0.5$ ,  $\rho_1 = 0.8$ .

The disturbed problem was solved by the reduction method with  $N = 15$  for different values of cylinder height  $2b$  and for both eigenstrain functions (32). Some results, obtained for  $b = 0.25, 0.5, 0.75, 1, 2$  (curves 1 to 5 correspondingly), are shown in Figs. from 2 to 5. The cases a) and b) correspond to the continuous and piecewise homogeneous eigenstrain radial distributions (33). The graphs in Figs. 2 show the distributions upon axial coordinate  $z$  of dimensionless total residual stress  $\sigma_{\rho\rho} = \sigma_{\rho\rho}^0 + \hat{\sigma}_{\rho\rho}$  at  $\rho = 0$ . The graphs in Figs. 3 and 4 show the distributions of dimensionless total residual stress components  $\sigma_{\varphi\varphi} = \sigma_{\varphi\varphi}^0 + \hat{\sigma}_{\varphi\varphi}$  and  $\sigma_{zz} = \sigma_{zz}^0 + \hat{\sigma}_{zz}$  on the lateral surface  $\rho = 1$  of the cylinder. Fig. 5 presents the distributions of residual stress component  $\sigma_{\rho z} = \hat{\sigma}_{\rho z}$  along the direction  $\rho = 0.5$ .

The conducted numerical analysis of residual stresses in a finite cylinder has shown that the height of the cylinder can considerably affect their distributions in the body bulk. Under increasing of the height  $2b$ , one can observe the edge effect in stress distributions, in particular, when  $b > 1$ , the residual stresses are quickly vary nearby the cylinder's bases and tend to the homogeneous values, specific for the initial state, in the domain remote from the bases.



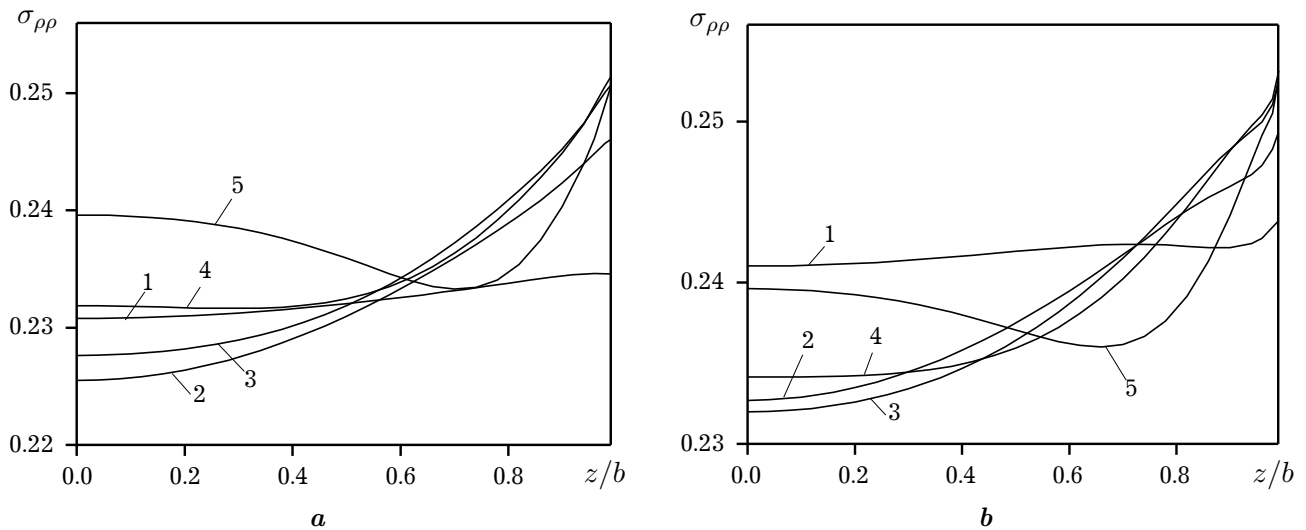


**Fig. 2.** Axial dependencies of stress component  $\sigma_{\rho\rho}$  at  $\rho = 0$  for the cases of continuous (a) and piece-wise homogeneous (b) eigenstrain functions  $\hat{e}(\rho)$ .

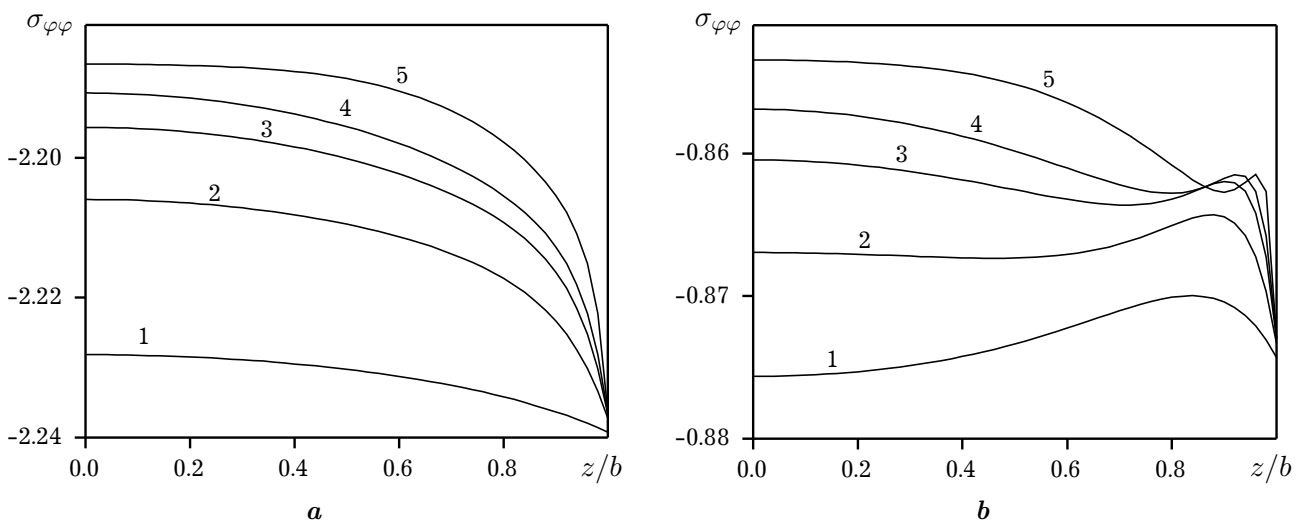


**Fig. 3.** Axial dependencies of stress component  $\sigma_{\varphi\varphi}$  at  $\rho = 1$  for the cases of continuous (a) and piece-wise homogeneous (b) eigenstrain functions  $\hat{e}(\rho)$ .

## 5. The model for probing of the body by polarized light

Photoelasticity is one of the most effective nondestructive techniques for obtaining empirical information about strain-stressed state of solids [1, 2]. It is based on interaction of polarized light with anisotropic medium, optical anisotropy of which is induced by its stress-strained state. The method is implemented by transillumination of the object with polarized light. The domain of application of this high-precision technique is potentially wider of class of bodies transparent in visible spectrum. Many materials, such as some dielectrics, semiconductors, plastics are transparent in infrared region.

Consider the application of the photoelasticity method for gathering of empirical information about axisymmetric strain-stressed state of the cylinder.

In Fig. 6, the transillumination of the object 1 with polarized light ray 2, emitted by the source 3, is shown. To prevent scattering of the ray by the surface, the object 1 is immersed into the liquid 4, the refractive index of which is very close to refractive index of the object (the dashed curve shows the fluid level in a vessel).

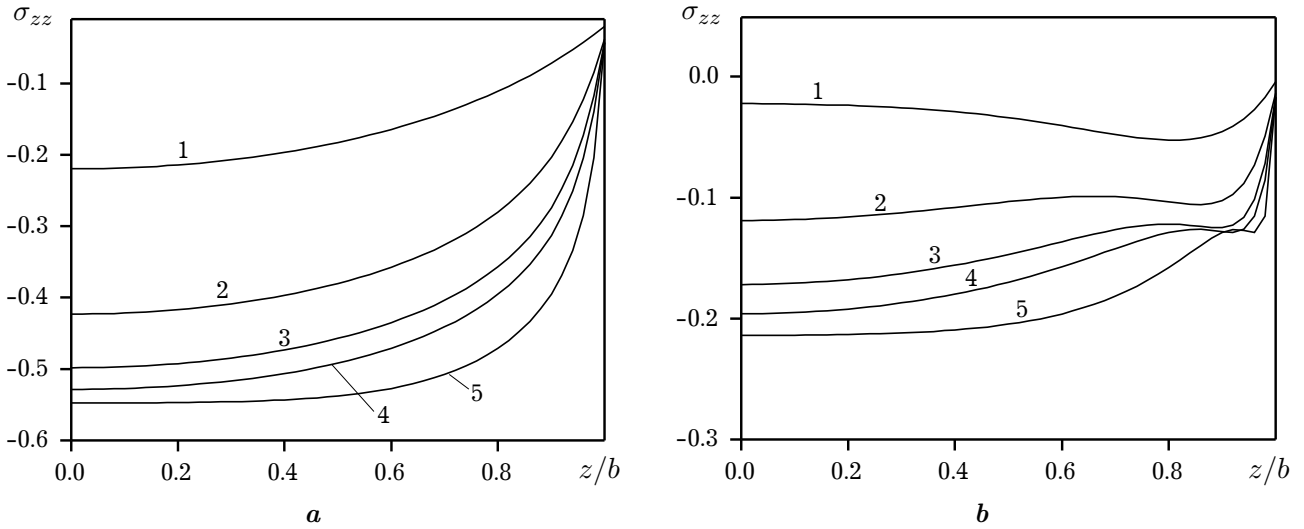


**Fig. 4.** Axial dependencies of stress component  $\sigma_{zz}$  at  $\rho = 1$  for the cases of continuous (a) and piece-wise homogeneous (b) eigenstrain functions  $\hat{\epsilon}(\rho)$ .

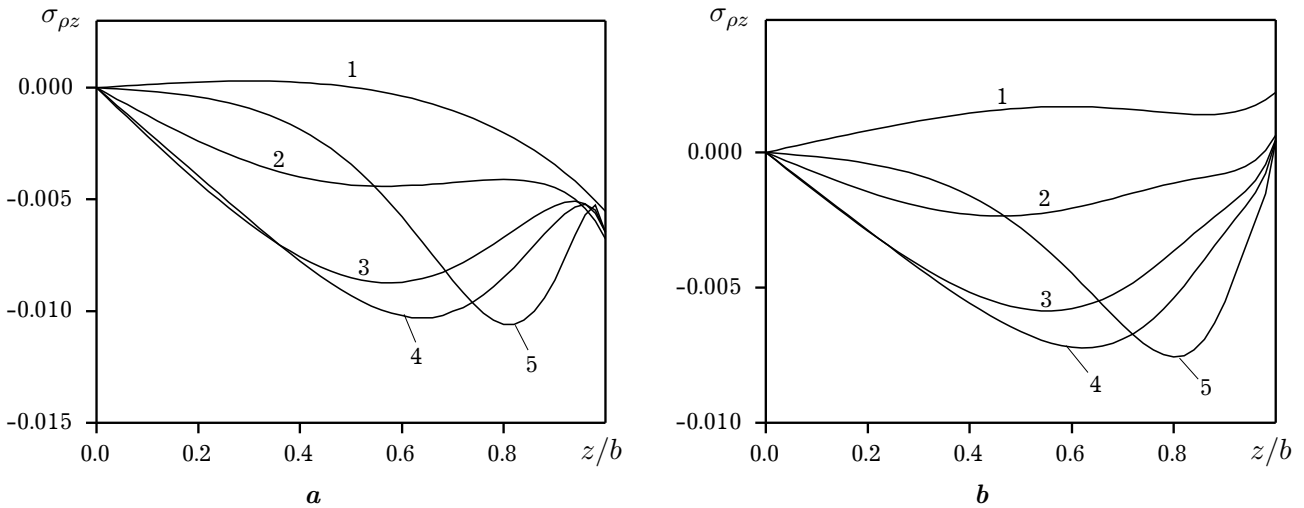


**Fig. 5.** Axial dependencies of stress component  $\sigma_{\rho z}$  at  $\rho = 0.5$  for the cases of continuous (a) and piece-wise homogeneous (b) eigenstrain functions  $\hat{\epsilon}(\rho)$ .

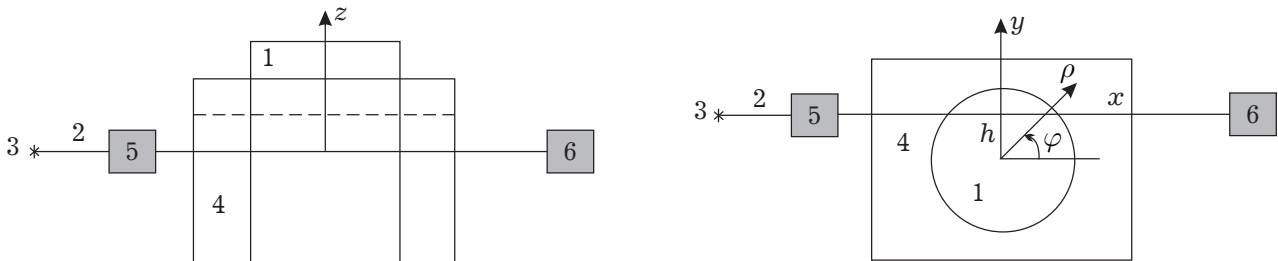


**Fig. 6.** Object probing schema.

All probing rays lay in the plane  $z = 0$ , hence they cross the cylinder perpendicularly to the axis  $z$ . A polarizer 5 forms the necessary input polarization of the ray. Any sounding direction is defined by its distance  $h$  from the origin of the coordinate system (see Fig. 6). Traveling through the object 1 in optically anisotropic medium, the ray changes its polarizations in conformity with distributions of strain tensor components 3 along its path. An analyzer 6 determines the output polarization of the ray.

Comparing the input and output polarizations of the ray, one can obtain some integral information about parameters of strain-stressed state along the ray.

Propagation of polarized light within the body is described by the models of integrated photoelasticity [5, 6]. It establishes a linear system of ordinary differential equations, describing variation of polarization state along the path of light ray propagation in strained medium. Coefficients of this system are dependent on parameters of strain-stressed state on this path. Since the probing ray lays in the plane of symmetry of strain-stressed state ( $z = 0$ ), the stress component  $\sigma_{\rho z}$  vanishes on it ( $\sigma_{\rho z}|_{z=0} = 0$ ), therefore, in the considered case (32) of isotropic eigenstrain tensor, the coefficients become dependent only on the components  $\sigma_{yy}$  and  $\sigma_{zz}$ . Here  $\sigma_{yy}$  and  $\sigma_{zz}$  are Cartesian components of the residual stress tensor in the coordinate system  $x, y, z$ , axis  $x$  of which is oriented along the probing ray,  $y$  axis is normal to both the ray and axis  $z$  of global coordinate system  $\rho, \varphi, z$ . In this case the system can be integrated in quadratures and one can obtain the integral relation [5]:

$$\delta = C \int_{x_{in}}^{x_{out}} (\sigma_{zz}|_{z=0} - \sigma_{yy}|_{z=0}) dx, \quad (34)$$

which expresses the phase difference  $\delta$ , acquired by polarized light ray on its way in strained medium, via the integral of residual stress components. Here  $C$  is a photoelasticity constant,  $x_{in}$ ,  $x_{out}$  are coordinates of the input and output points of the ray:

$$x_{in} = -\sqrt{1-h^2}, \quad x_{out} = \sqrt{1-h^2}. \quad (35)$$

By expressing in the formula (34) the Cartesian stress component via cylindrical ones, one can rewrite it in the form

$$\delta(h) = C \int_{x_{in}}^{x_{out}} (\sigma_{zz}(\rho(x), 0) - (\sigma_{\varphi\varphi}(\rho(x), 0) - \sigma_{\rho\rho}(\rho(x), 0)) \cos^2(\varphi(x))) dx, \quad (36)$$

where

$$\rho(x) = \sqrt{h^2 + x^2}, \quad \varphi(x) = \arccos \frac{x}{\sqrt{h^2 + x^2}}.$$

Using the solution of the direct problem, one can calculate by the formula (34) the phase difference  $\delta$ , acquired by the probing ray, depending on the direction (defined by the distance  $h$ ) of its propagation in the object. Such dependences, calculated on the solutions of the direct problem, obtained for eigenstrain representation in form (33)<sub>1</sub> and various  $b = 0.25, 0.5, 0.75, 1$  and  $2$  (curves 1 to 5 correspondingly) are shown in Fig. 7.

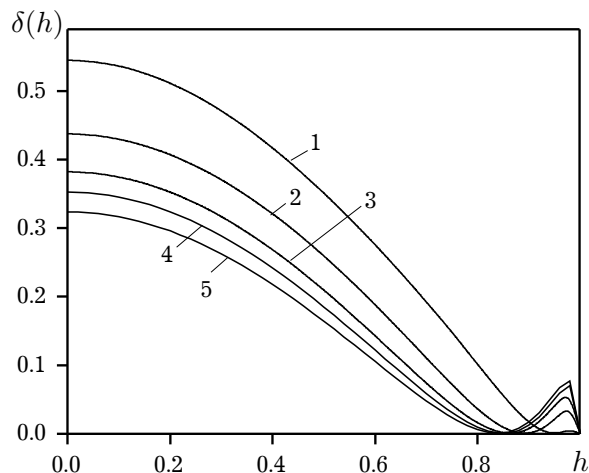


Fig. 7. The phase difference  $\delta$  depending on the direction  $h$ .

## 6. The inverse problem for residual stress determination and a method for its solving

### 6.1. Variational formulation of the inverse problem

The inverse problem consists in determination of the residual stresses in the cylinder in the case, when the function  $\hat{\varepsilon}(\rho)$  of eigenstrain is unknown. The direct problem in this case becomes underdetermined.

To compensate the deficient information, we will use empirical data, obtained through scanning the object by polarized light rays at its cross-section  $z = 0$  as it is shown in Fig. 6. Having made this, we obtain the empirical dependence  $\delta^e(h)$  similar to the curves shown in Fig. 7.

One can juxtapose the empirical function  $\delta^e(h)$  with its mathematical model, given by the formula (34), with the use of the functional of unknown function  $\hat{e}(\rho)$ :

$$\Phi(\hat{e}(\rho)) = \int_0^1 \left( \delta^e(h) - C \int_{x_{in}}^{x_{out}} (\sigma_{zz}|_{z=0} - (\sigma_{\varphi\varphi}|_{z=0} - \sigma_{\rho\rho}|_{z=0}) \cos^2\varphi) dx \right)^2 dh, \quad (37)$$

in which  $\sigma_{zz}$ ,  $\sigma_{\rho\rho}$  and  $\sigma_{\varphi\varphi}$  are residual stress components determined from the solution of the direct problem, corresponding to the arbitrary function  $\hat{e}(\rho)$ .

As we can see, under some restrictions on the class of permissible functions  $\hat{e}(\rho)$ , closer the function  $\hat{e}(\rho)$  to real eigenstrain distribution in the object is, the less should be the value of the integral calculated on the solution of direct problem for chosen  $\hat{e}(\rho)$ . Hence, we can search the function  $\hat{e}(\rho)$  as

$$\hat{e}(\rho) = \arg \min_{\hat{e}(\rho)} \Phi, \quad (38)$$

what leads to the variational problem:

$$\frac{\delta\Phi}{\delta\hat{e}(\rho)} = 0. \quad (39)$$

Taking into account additional posteriori information about the conditions under which the residual stresses were formed in the body one can substantially narrow the class of seeking function  $\hat{e}(\rho)$ . For instance, when the residual stress state of the body arose as result of hardening process, the eigenstrain distribution can be approximated by the formula

$$\hat{e}_{\rho\rho}(\rho) = \hat{e}_{\varphi\varphi}(\rho) = \hat{e}_{zz}(\rho) = \hat{e}_0 \exp\left(\frac{\rho-1}{a}\right), \quad (40)$$

where  $\hat{e}_0$  and  $a$  are unknown parameters, liable to the determination.

Such assumption appreciably simplifies the problem (39), since the functional (37) becomes a function of two variables  $\Phi = \Phi(\hat{e}_0, a)$  and we can find the parameters  $\hat{e}_0$  and  $a$  by solving system of two equations, which follow from necessary conditions of the function  $\Phi(\hat{e}_0, a)$  minimum:

$$\frac{\partial\Phi}{\partial\hat{e}_0} = 0, \quad \frac{\partial\Phi}{\partial a} = 0. \quad (41)$$

## 6.2. Numerical study of the solution of the inverse problem

To study computational feasibility of the developed method, we used a numeric experiment. For that we put in the formula (40)  $\hat{e}_0 = 2$  and  $a = 0.1$ . Than we solve the direct problem (the initial and disturbed ones), determine by the formula (30) the components of total stress tensor and calculate by the formula (36) the phase difference  $\delta(h)$ , which polarized light ray acquires during probing of cross-section  $z = 0$  of the object in dependence on distance  $h$  (see Fig. 7). Further we use such obtained function  $\delta(h)$  as empirical data  $\delta^e(h)$  for solving the inverse problem. Comparing both values  $\hat{e}_0$  and  $a$ , obtained by solving of the inverse problem, with those ones have been used in the direct problem when the “empirical data” have been obtained, one can evaluate the precision of the obtained solution of the inverse problem.

The dependence of the functional  $\Phi$  on  $\hat{e}_0$  and  $a$  are shown in Fig. 8 (curves a) and b) correspondingly). Curves 1 to 3 in the figure 8 a) calculated for the fixed values  $a = 0.09976, 0.09998, 0.1002$ , in Fig. 8 b) — for the fixed values  $\hat{e}_0 = 1.9976, 1.9998, 2.002$ . “Empirical data”, used in the functional (37), were obtained for  $\hat{e}_0 = 2$  and  $a = 0.1$ .

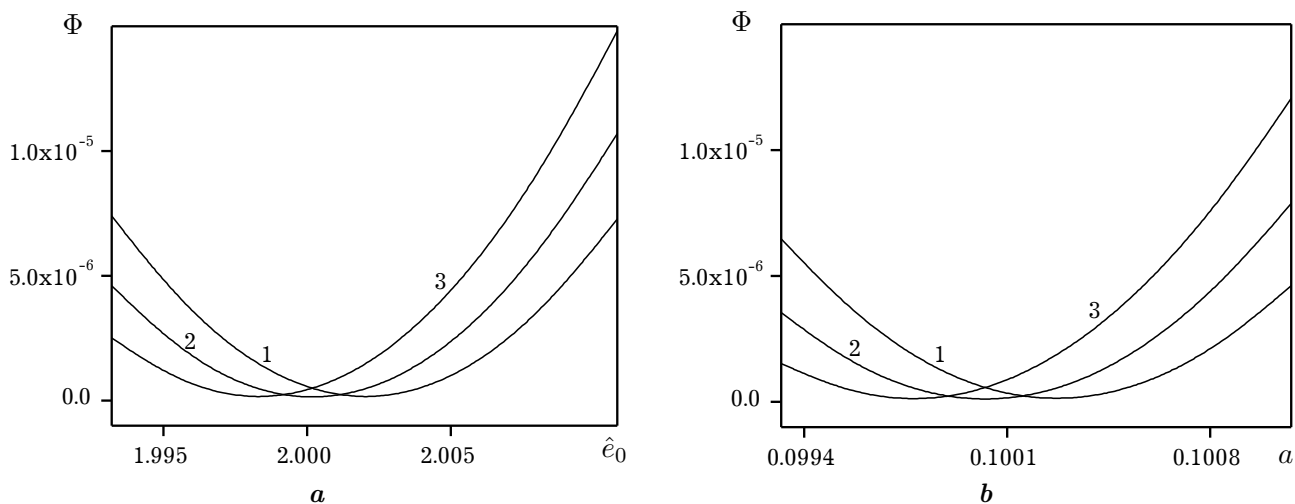


**Fig. 8.** Functional  $\Phi$  dependence on the  $\hat{e}_0$  (a) and  $a$  (b).

### 6.3. Solving the inverse problem

Let  $E_1^{(0)}$ ,  $E_2^{(0)}$  and  $A_1^{(0)}$ ,  $A_2^{(0)}$  be real numbers, which determine closed intervals  $E^{(0)} = (E_1^{(0)}, E_2^{(0)})$  and  $A^{(0)} = (A_1^{(0)}, A_2^{(0)})$  within which the sought for parameters  $\hat{e}_0$  and  $a$  take their values:  $\hat{e}_0 \in E^{(0)}$ ,  $a \in A^{(0)}$ .

We solve the inverse problem by iterative calculation of the value of the criterion functional (37).

For that, we partition the domain  $D^{(0)} = E^{(0)} \times A^{(0)}$  into  $n \times n$  equal subdomains  $D_{tq}^{(1)} = E_t^{(1)} \times A_q^{(1)}$ ,  $t = 1, 2, \dots, n$ ,  $q = 1, 2, \dots, n$  and calculate values  $\Phi_{tq}^{(1)}$  of the functional in the center of each subdomain. Then we find the value  $\Phi^{(1)} = \min_{tq} \Phi_{tq}^{(1)}$  and subdomain  $D^{(1)} = \arg \min_{tq} \Phi_{tq}^{(1)}$  in which the functional (37) is minimal. The found subdomain  $D^{(1)}$ , in turn, is partitioned into  $n \times n$  equal subdomains  $D_{tq}^{(2)}$  and so on. The iterative process is interrupted when the condition  $|\Phi^{(\lambda+1)} - \Phi^{(\lambda)}| \leq \varepsilon_\Phi$  is satisfied, where  $\varepsilon_\Phi$  is a given positive number,  $\lambda$  stands for the iteration number,  $\Phi^{(0)}$  is the value of the functional at the center of the domain  $D^{(0)}$ .

To study the feasibility of the presented algorithm, we acted as in previous subsection and, using the same values of the parameters  $\hat{e}_0 = 2$  and  $a = 0.1$ , determined the “empirical data”. The obtained on this basis functional (37) was minimized on the grid  $9 \times 9$ . After the second iteration errors of the inverse problem solution, determined as  $\varepsilon_{\hat{e}_0}^{(2)} = |\hat{e}_0^{(2)} - \hat{e}_0|$ ,  $\varepsilon_a^{(2)} = |a^{(2)} - a|$  was  $\varepsilon_{\hat{e}_0}^{(2)} = 0.002$ ,  $\varepsilon_a^{(2)} = 0.0002$ .

As we can see, iterative process of direct minimization of the function  $\Phi(\hat{e}_0, a)$ , rather quickly converges. Of course, one can use more sophisticated methods for solving the variational problem, in particular, those based on the Newton method [13].

## 7. Conclusions

The direct and inverse problems for nondestructive determination of axisymmetric residual stresses in a finite circular cylinder have been considered. The residual stresses are modeled with the use of the conception of eigenstrain. The consideration is restricted by the case of diagonal eigenstrain tensor, components of which are dependent only on a radial coordinate.

The direct problem is reduced to sequential solving of two problems. The first one is an axisymmetric problem for infinite cylinder, in which components of the eigenstrain tensor are prescribed as functions of radial coordinate. Its solution determines the initial stress state. The second problem determines the disturbance of the initial stress state, caused by the free surface of the finite cylinder's

bases. It consists in determination of elastic stresses in the finite cylinder, caused by tractions applied to its bases, when the lateral surface is free of load. This problem is solved with the use of variational method of homogeneous solutions.

In the inverse problem, the eigenstrain components are unknown and supposed to be functions of a radial coordinate. The information lack is compensated by data obtained by probing the body with polarized light ray. Variational formulation of the inverse problem have been made with the use of model of integrated photoelasticity. A method of its solving with the use of variational method of homogeneous solutions is developed. Eligibility of the developed methods for both direct and inverse problem has been studied quantitatively for two types of eigenstrains distributions in the cross-section of the body: continuous and piecewise homogeneous ones. The results show good convergence for the both types of distribution.

This approach can be expanded for case of eigenstrain tensor dependent on two coordinates — the radial and axial ones. The developed mathematical models and methods can be used, in particular, for nondestructive determination of residual stresses, originating in cylindrical bodies during their thermal treating.

- 
- [1] Schajer G. S. Practical residual stress measurement methods. John Wiley & Sons, Ltd (2013).
  - [2] Dally J. W., Riley W. F. Experimental stress analysis. McGraw-Hill, New York; 3rd edition (1991).
  - [3] Chekurin V. F. A variational method for solving of the problems of tomography of the stressed state of solids. *Materials Science*. **35** (5), 623–633 (1999).
  - [4] Chekurin V. F. An approach to solving of stress state tomography problems of elastic solids with incompatibility strains. *Mechanics of Solids*. **35** (6), 29–37 (2000).
  - [5] Aben H. Integrated Photoelasticity. McGraw-Hill, New York (1979).
  - [6] Chekurin V. F. Integral photoelasticity relations for inhomogeneously strained dielectrics. *Mathematical Modeling and Computing*. **1** (2), 144–155 (2014).
  - [7] Mura T. Micromechanics of Defects in Solids. Martinus Nijhof Publishers, Dordrecht, The Netherlands; 2nd edition (1987).
  - [8] Chekurin V. F., Postolaki L. I. A variational method of homogeneous solutions for axisymmetric elasticity problems for cylinder. *Mathematical Modeling and Computing*. **2** (2), 128–139 (2015).
  - [9] Chekurin V. F., Postolaki L. I. Application of variational method of homogeneous solutions for optimal control of axisymmetric thermoelastic state of cylinder. *Mathematical methods and physico-mechanical fields*. **60** (2), 105–116 (2017).
  - [10] Saad H. M. Elasticity. Theory, Applications and Numerics. Elsevier Academic Press (2005).
  - [11] Chekurin V., Postolaki L. Application of the least square method in axisymmetric biharmonic problems. *Mathematical Problems in Engineering*. **2016**, Article ID 3457649, 9 pages (2016).
  - [12] Kantorovich L. V., Krylov V. I. Approximate methods of higher analysis. Translated from the 3rd Russian Edition by C. D. Benster. Interscience Publ., New York (1958).
  - [13] Dennis J. E., Schnabel R. B. Numerical methods for unconstrained optimization and nonlinear equations. Prentice-Hall Inc., New Jersey (1983).

## Залишкові напруження в скінченному циліндрі. Пряма й обернена задачі та їх розв'язування з використанням варіаційного методу однорідних розв'язків

Чекурін В., Постолакі Л.

*Інститут прикладних проблем механіки і математики ім. Я. С. Підстригача НАН України,  
вул. Наукова, 3-б, Львів, 79060, Україна*

Розглянуто математичні моделі та методи визначення осесиметричних залишкових напружень у скінченному циліндрі. З використанням концепції вільних несумісних деформацій побудовано модель залишкових напружень, в межах якої сформульовано пряму задачу для визначення залишкових напружень. У цій задачі компоненти вільних несумісних деформацій розглядаються як задані функції радіальної координати. Для розв'язування прямої задачі розроблено варіаційний метод однорідних розв'язків. З використанням розробленого методу вивчено особливості залишкових напружень, зумовлені кусково-постійним та неперервним розподілами вільних несумісних деформацій у циліндрі. Розглянуто також обернену задачу, в якій компоненти вільних несумісних деформацій є невідомими функціями. Запропоновано варіаційне формулювання цієї задачі в межах моделей залишкових напружень та інтегрованої фотопружності та розроблено методику її розв'язування. Результати, подані в роботі, можуть бути використані для розроблення методів і засобів для неруйнівного тестування й інженерної характеристики матеріалів та елементів конструкції.

**Ключові слова:** залишкові напруження, скінченний циліндр, фотопружність, пряма й обернена задачі, варіаційний метод однорідних розв'язків.

**2000 MSC:** 35J30

**УДК:** 539.3